Acta Crystallographica Section F
Structural Biology and Crystallization Communications
ISSN 1744-3091

Structure of SurE protein from *Aquifex aeolicus* VF5 at 1.5 Å resolution

Svetlana V. Antonyuk,[a] Mark J. Ellis,[b] Richard W. Strange,[a]* Yoshitaka Bessho,[c,d] Seiki Kuramitsu,[d,e] Akeo Shinkai,[d] Shigeyuki Yokoyama[c,d,f] and S. Samar Hasnain[a]*

[a]Molecular Biophysics Group, School of Biological Sciences, University of Liverpool, Crown Street, Liverpool L69 7ZB, England, [b]STFC Daresbury Laboratory, Warrington, Cheshire WA4 4AD, England, [c]Systems and Structural Biology Center, Yokohama Institute, RIKEN, 1-7-22 Suehiro, Tsurumi, Yokohama 230-0045, Japan, [d]RIKEN SPring-8 Center, Harima Institute, 1-1-1 Kouto, Sayo, Hyogo 679-5148, Japan, [e]Department of Biological Sciences, Graduate School of Science, Osaka University, 1-1 Machikaneyama, Toyonaka, Osaka 560-0043, Japan, and [f]Department of Biophysics and Biochemistry, Graduate School of Science, The University of Tokyo, 7-3-1 Hongo, Bunkyo-ku, Tokyo 113-0033, Japan

Correspondence e-mail: r.strange@liverpool.ac.uk, s.s.hasnain@liverpool.ac.uk

Received 25 June 2009
Accepted 22 October 2009

PDB Reference: SurE, 2wqk, r2wqksf.

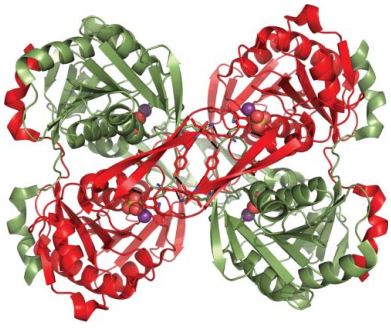

SurE is a stationary-phase survival protein found in bacteria, eukaryotes and archaea that exhibits a divalent-metal-ion-dependent phosphatase activity and acts as a nucleotidase and polyphosphate phosphohydrolase. The structure of the SurE protein from the hyperthermophile *Aquifex aeolicus* has been solved at 1.5 Å resolution using molecular replacement with one dimer in the asymmetric unit and refined to an *R* factor of 15.6%. The crystal packing reveals that two dimers assemble to form a tetramer, although gel-filtration chromatography showed the presence of only a dimer in solution. The phosphatase active-site pocket was occupied by sulfate ions from the crystallization medium.

1. Introduction

The SurE gene is part of a stationary-phase survival operon that is found in eubacteria, eukaryotes and archaea and which is induced in cells during high levels of stress or slow growth (Li *et al.*, 1997; Visick *et al.*, 1998). Biochemical characterization of the SurE protein in *Escherichia coli* shows it to be a divalent metal ion-dependent phosphatase with both nucleotidase and exopolyphosphatase activity (Proudfoot *et al.*, 2004). Initial evidence for phosphatase activity in the SurE family has been provided together with the first crystal structures of the enzyme from the bacterium *Thermotoga maritima* (Lee *et al.*, 2001; Zhang *et al.*, 2001). Subsequently, crystal structures of archaeal SurE from *Pyrobaculum aerophilum* (Mura *et al.*, 2003) and SurE from *Thermus thermophilus* (Iwasaki & Miki, 2007) have been published. Here, as a target in a high-throughput genomics study, we report the structure of recombinant SurE (*Aa*SurE) from *Aquifex aeolicus*, a hyperthermophilic bacterium found in hot springs with a growth temperature of 358–368 K (Huber & Stetter, 2001).

2. Materials and methods

2.1. Cloning, expression and purification

The gene encoding *Aa*SurE protein (aq_832; gi:15606188) was amplified *via* PCR using *A. aeolicus* VF5 genomic DNA and was cloned into pET-21a expression vector (Merck Novagen, Darmstadt, Germany). The expression vector was introduced into *E. coli* BL21-CodonPlus(DE3)-RIL strain (Stratagene, La Jolla, California, USA) and the recombinant strain was cultured in 4.5 l LB medium containing 30 µg ml^{-1} chloramphenicol and 50 µg ml^{-1} ampicillin. The harvested cells (19 g) were lysed by sonication in 35 ml 20 m*M* Tris–HCl buffer pH 8.0 containing 500 m*M* NaCl, 5 m*M* β-mercaptoethanol and 1 m*M* phenylmethylsulfonyl fluoride on ice. The cell lysate was heat-treated at 363 K for 12 min and centrifuged at 15 000*g* for 30 min at 277 K. The supernatant was desalted by fractionation on a HiPrep 26/10 column (GE Healthcare Biosciences). The sample was applied onto a Toyopearl SuperQ-650M column (Tosoh, Tokyo) equilibrated with 20 m*M* Tris–HCl buffer pH 8.0 and eluted with a linear (0–0.4 *M*) gradient of NaCl. The target sample, which eluted in the 0.18 *M* NaCl fraction, was then applied onto a Resource Q column (GE Healthcare Biosciences) equilibrated with 20 m*M* Tris–HCl buffer pH 8.0 and eluted with a linear gradient of 0–0.3 *M* NaCl.

Table 1
Data-collection and refinement parameters.

Values in parentheses are for the highest resolution shell (1.55–1.5 Å).

Space group	$P3_221$
Unit-cell parameters (Å)	$a = b = 65.01$, $c = 239.19$
Resolution (Å)	36.5–1.5
Unique reflections	86861
Completeness (%)	95.9 (68.2)
Redundancy	8.7 (2.1)
R_{merge}† (%)	8.1 (19.4)
$I/\sigma(I)$	22 (3)
R factor‡ (%)	15.6
R_{free}‡ (%)	19.1
B factors (Å^2)	
Wilson plot	19.8
Protein	15.7
Water	35.8
Na ion, chain A	16.7
Na ion, chain B	16.9
R.m.s. deviations	
Bond distances (Å)	0.015
Bond angles (°)	1.591
ESU§ (Å)	0.078

† $R_{merge} = \sum_{hkl}\sum_i |I_i(hkl) - \langle I(hkl)\rangle| / \sum_{hkl}\sum_i I_i(hkl)$, where $I_i(hkl)$ is the observed intensity and $\langle I(hkl)\rangle$ is the average intensity of multiple symmetry-related observations of that reflection. ‡ $R = \sum_{hkl} ||F_{obs}| - |F_{calc}|| / \sum_{hkl} |F_{obs}|$. R_{free} is the same but calculated for a test set not used in structural refinement. § Estimated standard uncertainty based on R factor as implemented in *REFMAC*.

The fractions that eluted in 0.14 *M* NaCl were further purified using a hydroxyapatite CHT20-I column (Bio-Rad Laboratories) with a linear gradient of 0.01–0.5 *M* potassium phosphate buffer pH 7.0. The target sample, which eluted in the 0.18 *M* potassium phosphate fraction, was collected and applied onto a HiLoad 16/60 Superdex 200pg column (GE Healthcare Biosciences) equilibrated with 20 m*M* Tris–HCl buffer pH 8.0 containing 200 m*M* NaCl. The protein sample was analyzed by SDS–PAGE and was confirmed by N-terminal amino-acid sequencing. After concentration to 27.8 mg ml^{-1} by ultrafiltration, the protein yield was 42.0 mg from 19 g of cells.

2.2. Crystallization

Crystallization was performed by the microbatch-under-oil method at 291 K. 0.5 µl crystallization regent, consisting of 0.1 *M* acetate buffer pH 4.5 containing 2.5 *M* NaCl and 0.2 *M* Li_2SO_4 (Wizard II condition No. 38; Emerald BioSystems), was mixed with 0.5 µl 27.8 mg ml^{-1} protein solution. The mixture was then covered with 15 µl silicone and paraffin oil. Crystals suitable for X-ray data collection appeared within three weeks and reached final dimensions of 0.2 × 0.2 × 0.03 mm (Fig. 1). The crystals were flash-cooled in a nitrogen-gas stream at 100 K using 20%(*v*/*v*) glycerol as a cryoprotectant for transport to the synchrotron.

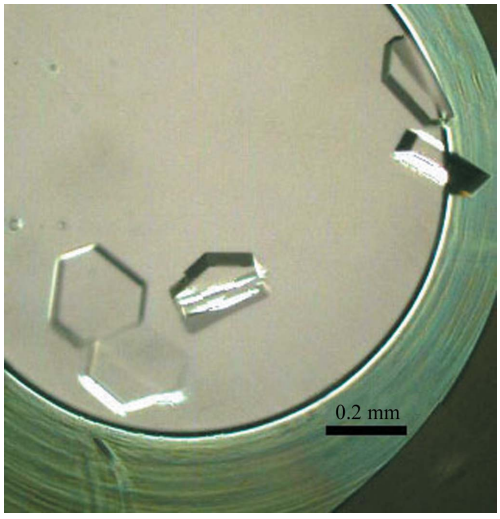

Figure 1
Crystals of *A. aeolicus* VF5 SurE.

2.3. Data collection and processing

Experiments were performed at the Daresbury Synchrotron Radication Source (SRS) using the combined crystallography/X-ray absorption beamline 10.1, employing a Si(111) sagittally focused monochromator tuned to a wavelength of 1.04 Å. Diffraction data were recorded at 100 K from a single SurE crystal immersed in reservoir solution with 20% glycerol added as a cryoprotectant. The first image showed evidence in the low-resolution data of the presence of partially ordered ice in the crystal. The initial diffraction resolution was improved by 0.5 Å by annealing the crystal (Ellis *et al.*, 2002), a procedure that also removed the ice rings and reduced the mosaic spread to 0.28°. Images were recorded using a MAR Mosaic 225 CCD detector and were processed (indexed, integrated and scaled) using *HKL*-2000 (Otwinowski & Minor, 1997). The crystal was found to belong to space group $P3_221$, with unit-cell parameters $a = b = 65.01$, $c = 239.19$ Å. The estimated solvent content was 52% for two molecules in the asymmetric unit.

2.4. Structure solution and refinement

The structure was solved by molecular replacement with *MOLREP* (Vagin & Teplyakov, 1997), using as a search model SurE from *Thermotoga maritima* with 42% identity and 69% similarity to the target sequence and consisting of one subunit of entry 1j9j (Lee *et al.*, 2001) from the Protein Data Bank (Abola *et al.*, 1987). To facilitate structure solution, the search model was truncated by removing the protruding β-hairpin and α-helix belonging to the C-terminus. The initial R factor for two molecules in the asymmetric unit was poor at only 61%, necessitating significant rebuilding with *Coot* (Emsley & Cowtan, 2004) during successive cycles of refinement using *REFMAC* (Murshudov *et al.*, 1997). As the electron-density maps improved, the sequence for *A. aeolicus* was gradually introduced into the model to replace the sequence of *T. maritima*. Water molecules were added to the structure using *Coot*. The stereochemistry was checked using *PROCHECK* (Laskowski *et al.*, 1993). The Ramachandran plot showed 98.0% of residues to be in the core region and 2.0% to be in additionally allowed regions. The R factor and R_{free} for the final model were 15.6% and 19.1%, respectively. Table 1 summarizes the data-collection and refinement parameters. The stereochemistry of the final model was checked using *MolProbity* (Davis *et al.*, 2007). The structure was deposited in the PDB under accession code 2wqk. The protein interfaces, surfaces and assemblies service *PISA* (Krissinel & Henrick, 2007) at the European Bioinformatics Institute (http://www.ebi.ac.uk/msd-srv/prot_int/pistart.html) was used to calculate the molecular properties described below.

3. Results and discussion

The structure of *Aa*SurE was obtained at 1.5 Å resolution with one dimer (subunits *A* and *B*) in the asymmetric unit, comprising 4116 protein atoms, 605 water molecules, two sulfate ions and two sodium ions. For each subunit, 248 residues (of 251) were positioned in the electron-density maps, with only the N-terminal Met1 and C-terminal Ser250 and Pro251 residues missing from the final model. Each subunit comprises a core globular domain containing nine β-strands

and six helices in a Rossmann-like fold, with two extended segments at the C-terminal end: a 30-residue β-hairpin linking β-strands 8 and 11 and a 15-residue terminating α-helix, α8 (Fig. 2*a*). The C-terminal extensions are involved in forming the dimer. As in the previously reported structures of bacterial SurE from *Thermotoga maritima* (Lee *et al.*, 2001; Zhang *et al.*, 2001) and *Thermus thermophilus* (Iwasaki & Miki, 2007), domain swapping occurs at the C-terminal helix α8. These helices are well ordered in *Aa*SurE and are clearly traceable in the electron-density maps (Fig. 2*b*). Symmetry-related contacts at the dimer interface are provided by residues 40–54 (N-terminal loops), 100–113 (α3 and α4), 174–204 (β8 and β-hairpin) and 227–249 (β11 and α8), yielding a total of 20 salt bridges and more than 30 hydrogen bonds between the two subunits. Dimer formation encompasses up to 25% of the solvent-accessible surface area of each subunit. Experimental evidence from size-exclusion chromatography shows that *Aa*SurE exists as a dimer in solution, while analysis of the protein interfaces (Krissinel & Henrick, 2007) suggests that both dimeric and tetrameric quaternary structures are stable in solution.

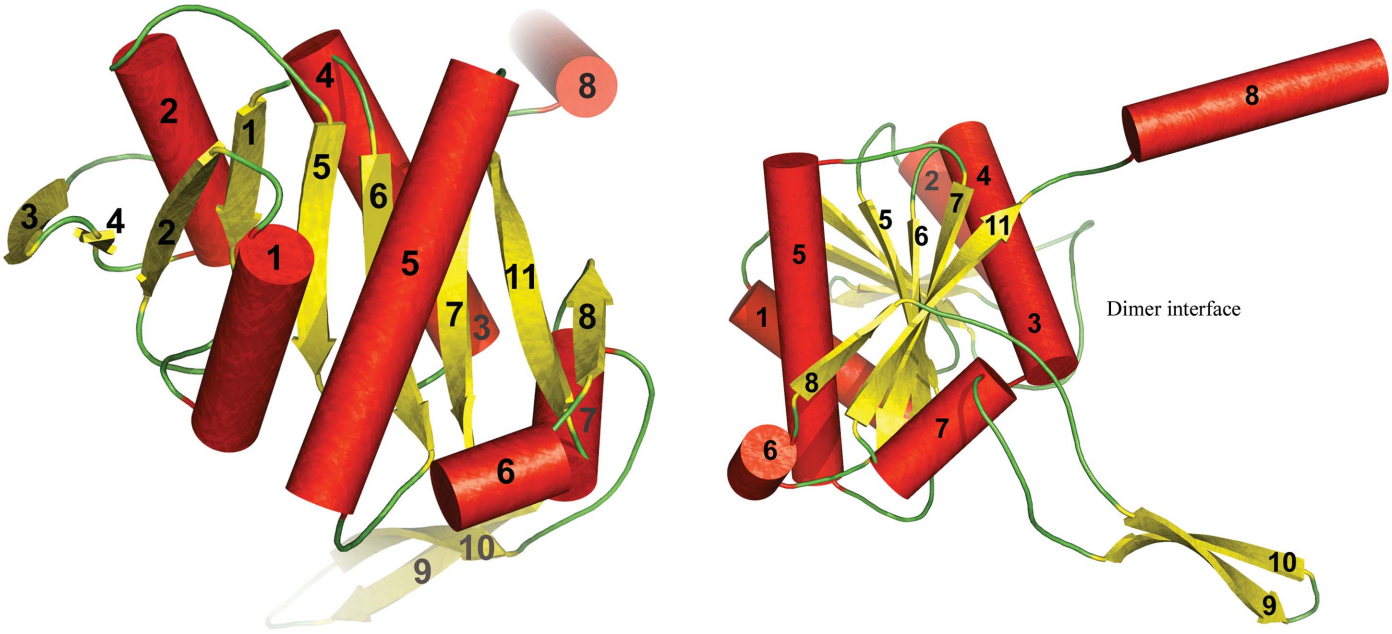

(*a*)

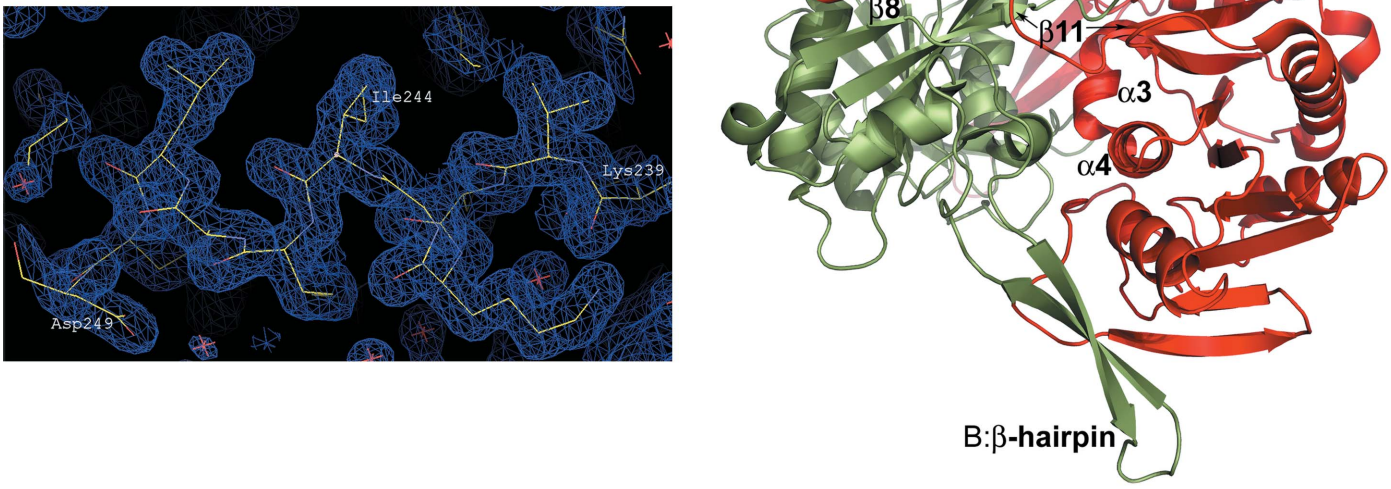

(*b*)

Figure 2
(*a*) Two orthogonal orientations of the *Aa*SurE subunit showing the secondary structure and overall fold. The core globular domain consists of nine β-strands (yellow) and six helices (red cylinders), with helix α7 linking the C-terminal β-hairpin to the main body of the molecule. The dimer interface is located on the subunit edge where the β-hairpin (strands β9 and β10) and helix α8 project away from the main body of the molecule. (*b*) The *Aa*SurE dimer (right) as found in the asymmetric unit, indicating the secondary-structure elements involved in forming salt bridges and/or hydrogen bonds between the two subunits *A* (red) and *B* (green). The domain-swapped α8 helices are well ordered. The quality of the electron-density map (left) is shown for *A* α8 at the 1σ contour level. The overall fold of *Aa*SurE compared with the SurE dimers from other organisms give root-mean-square deviations for C^{α} atoms of 2.9 Å (PDB code 1j9j, the molecular-replacement search model) and 2.6 Å for 1ilv (both from *Thermotoga maritima*), 2.1 Å for 1l5x from *P. aerophilum* and 6.7 Å for 2e6e from *Thermus thermophilus*. This figure was drawn using *Coot* (Emsley & Cowtan, 2004) and *PyMOL* (DeLano, 2008).

The biologically relevant molecular assembly in solution was initially identified as a dimer in *Thermotoga maritima* SurE (Lee *et al.*, 2001) and *P. aerophilum* SurE (Mura *et al.*, 2003), while a functional tetramer was proposed for *T. maritima* SurE on the basis of crystal packing and size-exclusion chromatography (Zhang *et al.*, 2001). More recently, *Thermus thermophilus* SurE has been crystallized with one or more tetramers in the asymmetric unit in space groups $P3_121$ and $P2_12_12_1$, with additional evidence for a dimer–tetramer equilibrium being obtained from sedimentation-equilibrium experiments (Iwasaki & Miki, 2007). A tetramer of *Aa*SurE, obtained by examining the crystal packing, is shown in Fig. 3(*a*). The two dimers interact primarily through contacts between the β-hairpins of adjacent subunits, interfaces A–A' and B–B', burying 4.8% of the solvent-accessible surface area of each subunit at each interface. Only eight additional potential hydrogen bonds are created at each interface by tetramerization. These observations suggest that the association of dimers into tetramers is relatively weak and may explain why only dimers were found in solutions of *Aa*SurE.

The divalent metal ion-binding site consists of residues that are highly conserved among SurE genes (Lee *et al.*, 2001). The preferred metal cofactor is Mg^{2+} in *Thermotoga maritima* (Lee *et al.*, 2001; Zhang *et al.*, 2001) and *Thermus thermophilus* (Iwasaki & Miki, 2007) and Co^{2+} in the hyperthermophilic *P. aerophilum* (Mura *et al.*, 2003). The locations of the four identical active sites in the *Aa*SurE tetramer are shown in Fig. 3(*a*). A superposition of the active sites of subunit *A* with those of *Thermotoga maritima*, *Thermus thermophilus* and *P. aerophilum* are shown in Fig. 3(*b*). In *Aa*SurE, the active-site pocket is occupied by a sulfate ion, presumably from the crystallization medium, with electron density at the metal-binding site adequate for modelling with either solvent or a metal ion.

We thank Mr Yoshiaki Kitamura and Dr Akio Ebihara for help in sample preparation. This work was supported in part by the RIKEN Structural Genomics/Proteomics Initiative (RSGI), the National Project on Protein Structural and Functional Analyses, Ministry of Education, Culture, Sports, Science and Technology of Japan. This work was supported by the Synchrotron Radiation Department at the Science and Technology Facilities Council, Daresbury Laboratory UK and X-ray data were collected on beamline 10.1 at the Synchrotron Radiation Source, which was supported by Biotechnology and Biological Sciences Research Council Grant BB/E001971 (to SSH and RWS).

References

Abola, A., Bernstein, F. C., Bryant, S. H., Koetzle, T. F. & Weng, J. (1987). *Crystallographic Databases – Information Content, Software Systems, Scientific Applications*, edited by F. H. Allen, G. Bergerhoff & R. Sievers, pp. 107–132. Bonn/Cambridge/Chester: Data Commission of the International Union of Crystallography.

DeLano, W. L. (2008). *PyMOL Molecular Viewer.* DeLano Scientific, Palo Alto, California, USA. http://www.pymol.org.

Ellis, M. J., Antonyuk, S. & Hasnain, S. S. (2002). *Acta Cryst.* D**58**, 456–458.

Emsley, P. & Cowtan, K. (2004). *Acta Cryst.* D**60**, 2126–2132.

Huber, R. & Stetter, K. O. (2001). *Methods Enzymol.* **330**, 11–24.

Iwasaki, W. & Miki, K. (2007). *J. Mol. Biol.* **371**, 123–136.

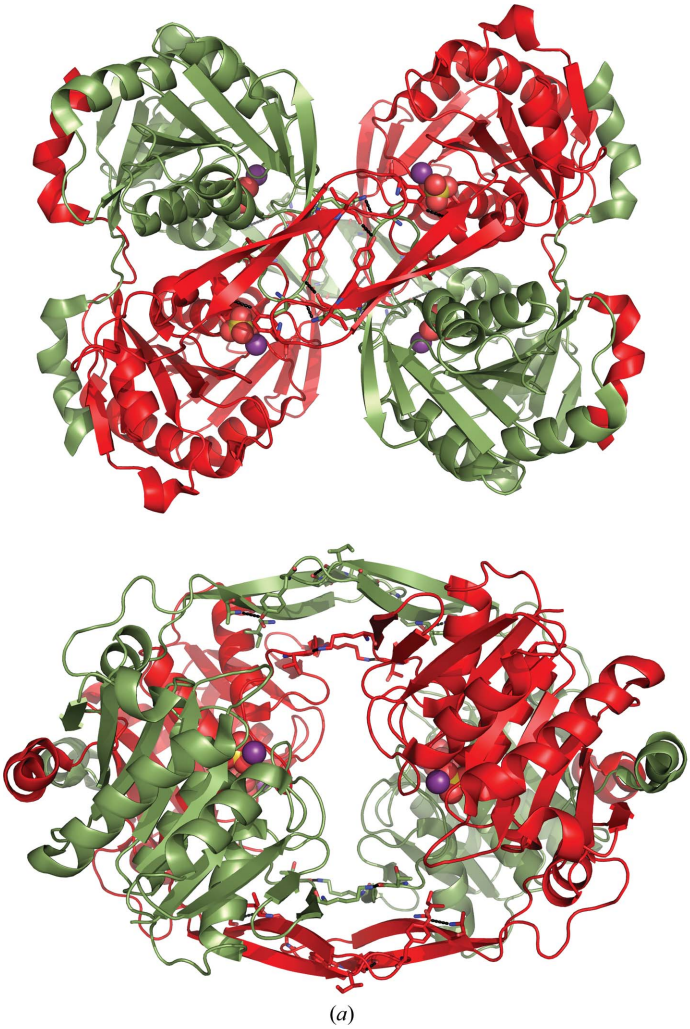

(*a*)

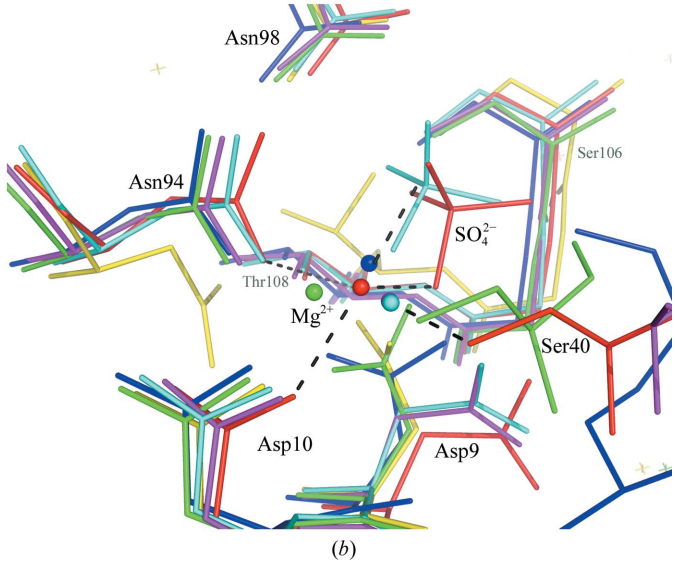

(*b*)

Figure 3
(*a*) A tetramer of *Aa*SurE, generated by applying symmetry operations to the dimer, is shown in two orthogonal views. The main contacts forming the tetramer interfaces occur between the β-hairpin strands of adjacent *A* (red) subunits and adjacent *B* (green) subunits. The metal-binding site that gives the enzyme its phosphatase activity is shown for each subunit, with a water molecule or Na ion (magenta sphere) occupying the position usually taken by a divalent metal ion and with a sulfate ion (red and yellow spheres) filling the active-site pocket. (*b*) Close-up of the active site of subunit *A* (red sticks) compared with the equivalent sites in SurE from *Thermotoga maritima* with Mg^{2+} (PDB entry 1j9j, green) or water (1ilv, magenta) at the metal-binding site, from *Thermus thermophilus* with water and a sulfate ion in the active site (2e69, cyan) or an empty active site (2e6e, yellow) and from *P. aerophilum* (1l5x, blue) with water at the active site. The numbering of the active-site ligands follows the sequence of *Aa*SurE.

Krissinel, E. & Henrick, K. (2007). *J. Mol. Biol.* **372**, 774–797.
Laskowski, R. A., MacArthur, M. W., Moss, D. S. & Thornton, J. M. (1993). *J. Appl. Cryst.* **26**, 283–291.
Lee, J. Y., Kwak, J. E., Moon, J., Eom, S. H., Liong, E. C., Pedelacq, J. D., Berendzen, J. & Suh, S. W. (2001). *Nature Struct. Biol.* **8**, 789–794.
Li, C., Wu, P. Y. & Hsieh, M. (1997). *Microbiology*, **143**, 3513–3520.
Davis, I. W., Leaver-Fay, A., Chen, V. B., Block, J. N., Kapral, G. J., Wang, X., Murray, L. W., Arendall, W. B. III, Snoeyink, J., Richardson, J. S. & Richardson, D. C. (2007). *Nucleic Acids Res.* **35**, W375–W383.
Mura, C., Katz, J. E., Clarke, S. G. & Eisenberg, D. (2003). *J. Mol. Biol.* **326**, 1559–1575.
Murshudov, G. N., Vagin, A. A. & Dodson, E. J. (1997). *Acta Cryst.* D**53**, 240–255.
Otwinowski, Z. & Minor, W. (1997). *Methods Enzymol.* **276**, 307–326.
Proudfoot, M., Kuznetsova, E., Brown, G., Rao, N. N., Kitagawa, M., Mori, H., Savchenko, A. & Yakunin, A. F. (2004). *J. Biol. Chem.* **279**, 54687–54694.
Vagin, A. & Teplyakov, A. (1997). *J. Appl. Cryst.* **30**, 1022–1025.
Visick, J. E., Ichikawa, J. K. & Clarke, S. (1998). *FEMS Microbiol. Lett.* **167**, 19–25.
Zhang, R.-G., Skarina, T., Katz, J. E., Beasley, S., Khachatryan, A., Vyas, S., Arrowsmith, C. H., Clarke, S., Edwards, A., Joachimiak, A. & Savchenko, A. (2001). *Structure*, **9**, 1095–1106.